A900 2455
2974

Nuclear Instruments and Methods in Physics Research B80/81 (1993) 653–658
North-Holland

NIM B
Beam Interactions
with Materials & Atoms

Optical doping of silicon with erbium by ion implantation

A. Polman, J.S. Custer, E. Snoeks and G.N. van den Hoven
FOM-Institute for Atomic and Molecular Physics, Kruislaan 407, 1098 SJ Amsterdam, The Netherlands

New procedures to incorporate high concentrations of erbium in silicon are presented, together with measurements of the characteristic photoluminescence at 1.5 μm of Er^{3+} in silicon. Er-doped amorphous Si was prepared by implantation of 5.4×10^{15} Er/cm^2 at 250 keV into 550 nm thick amorphous Si surface layers prepared by Si implantation. The incorporation of Er in crystalline Si was investigated for Si(100) implanted with 250 keV Er at 9×10^{14} cm^{-2}. The amorphized Si layers were crystallized by either thermal solid phase epitaxy (SPE) at 600°C, or ion beam induced epitaxial crystallization (IBIEC) at 250°C. Segregation of Er is observed during SPE, with Er concentrations up to 10^{20} cm^{-3} remaining trapped in the crystal ($\chi_{min} \approx 5\%$) after regrowth. Under IBIEC, the original Er profile is completely trapped in the crystal ($\chi_{min} \approx 10\%$). Thermal annealing was used to optically activate the Er. After annealing at 400°C, the Er-doped amorphous Si layers show a very small photoluminescence intensity (at 77 K) around 1.5 μm, superimposed on a defect band from the amorphous Si itself. For samples crystallized by SPE or IBIEC the maximum photoluminescence signal (at 77 K) is obtained after annealing at 1000°C. The intensities are much higher than for Er in amorphous Si. SPE regrown samples show sharp spectra peaked at 1.54 μm, while IBIEC samples exhibit a broad spectrum, ≈ 0.1 μm wide, peaked at 152 μm. The similarities and differences in optical spectra for the different Er-doped materials are discussed.

1. Introduction

Silicon is the key element in today's electronic integrated-circuit technology. Unfortunately, Si has an indirect band gap, which precludes efficient light emission under electrical excitation. Since optical technologies are becoming more important in areas that were traditionally the domain of electronics [1], it becomes more and more important to find solutions around this problem. Several efforts have been made already to obtain light emission from silicon: band gap engineering by the addition of Ge or the addition of isoelectronic impurities or structural defects resulting in radiative recombination. However, none of these methods have proven successful. Ennen et al. [2,3] have pointed out the potential of rare-earth ions in semiconductor materials for obtaining light emission. Rare-earth ions, incorporated in the proper charge state, have internal luminescent intra-4f transitions, which are shielded from the surrounding crystal by filled outer electron shells.

Fig. 1 shows a schematic energy level diagram of the rare-earth erbium in its trivalent state. The levels are determined by the Coulomb interaction and spin-orbit coupling for the 4f electrons. For Er incorporated in a solid, the local electric field lifts the degeneracy of these levels (Stark splitting). Each level splits up in a manifold of which the exact line positions depend on the field strength and Er site symmetry. The lines broaden by inhomogeneities in Er site distribution, as well as homogeneous broadening (at elevated temperatures). An important effect of the crystal field is that it modifies the transition probabilities between the Er^{3+} manifolds so that some transitions, which are forbidden in the free ion, become allowed. The transition between the first excited manifold $^4I_{13/2}$ and the ground manifold $^4I_{15/2}$ is of great interest because it occurs at a wavelength of 1.5 μm, a standard wavelength in telecommunication technology. Photoluminescence [2–7] and electroluminescence [3] of this transition in Si:Er have indeed been demonstrated. The details of the excitation mechanism for luminescence are at present unknown. One possible mechanism involves the recombination of electron–hole pairs (generated either electrically or by optical pumping) near an Er ion. The recombination energy is then transferred to the Er ion, which then releases its energy by radiative or nonradiative decay to the ground state. Other excitation mechanisms have also been proposed [8]. In fig. 1, for reference, the magnitude of the Si band gap is indicated schematically.

Apart from limited work on Er-doped hydrogenated amorphous Si [9] most work in the past few years concentrates on Er incorporated in crystalline Si (c-Si). These studies include the optical spectra [2–7], the Er site configuration [5], the role of impurities on the luminescence [6,7] and the electrical properties [10–12]. Only very few studies have been made on the structural aspects of incorporating Er in c-Si [13–16]. At present, important questions as to the Er solubility, as well as diffusion and precipitation phenomena have remained unanswered and the optimum recipe for

0168-583X/93/$06.00 © 1993 – Elsevier Science Publishers B.V. All rights reserved

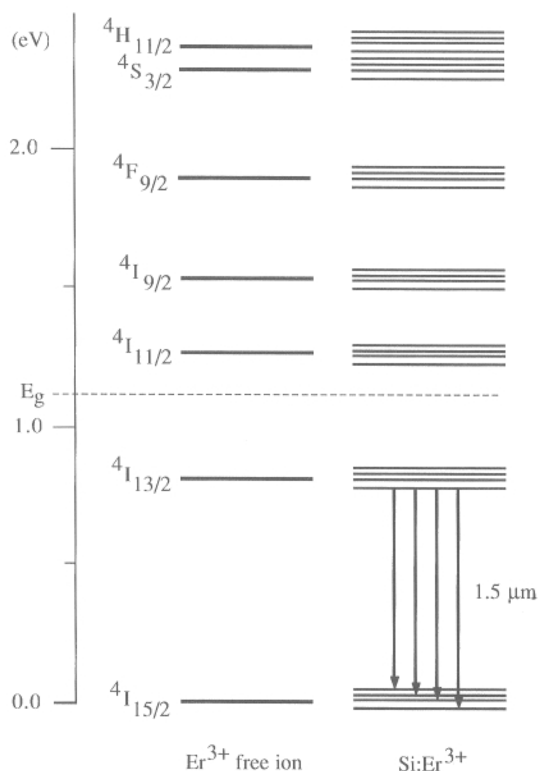

Fig. 1. Schematic energy level diagram for Er^{3+}. The scheme on the left indicates the different levels for the Er free ion, determined by Coulomb interaction and spin–orbit coupling for the 4f electrons. As indicated on the right, the Stark effect further splits these levels when Er is incorporated in a host such as Si. The main transitions of interest are indicated by arrows. The magnitude of the Si band gap is indicated schematically by the dashed line.

incorporating high concentrations of Er in c-Si is yet unknown.

In this paper we study the incorporation of Er in Si by ion implantation. We first present results on Er in pure amorphous Si (a-Si). High concentrations of Er can be incorporated in a-Si, but the Er PL intensity is relatively low. We then continue with Er in c-Si. It has been shown before that very small quantities of Er ($< 10^{18}$ cm^{-3}) can be incorporated in good-quality c-Si by ion implantation and made optically active [13]. Higher concentrations lead to high densities of implantation-induced lattice displacements, which on annealing lead to extended defects [17]. The critical fluence for this to occur is on the order of 10^{13} ions/cm^2 at an implantation energy of 500 keV. As we will show, a way around this problem is to use high-dose implants which fully amorphize the Si. The Er-doped a-Si layers are then crystallized using either thermal solid phase epitaxial recrystallization (SPE) [18] at 600°C or ion beam induced epitaxial crystallization (IBIEC) [19] at 250°C. While some efforts have been made in the past to crystallize Er-doped a-Si by SPE, most of these have led to defective crystal growth [13–16]. As we will show in this paper, perfect epitaxy can only be obtained for low annealing temperatures. The Er concentration incorporated by either SPE of IBIEC is as high as 10^{20} cm^{-3}. At 77 K, these Er-doped materials show clear photoluminescence from Er near 1.5 μm.

2. Experimental

Czochralski-grown (CZ) n-type (100)Si wafers with a resistivity of 1 Ω cm were used in all experiments. The a-Si:Er samples were prepared by first amorphizing a 550 nm thick Si surface layer with 3×10^{15} Si/cm^2 at 350 keV, followed by a 5.4×10^{15} Er/cm^2 Er implant at 250 keV. SPE and IBIEC studies were carried out on samples in which 9×10^{14} Er ions/cm^2 were directly implanted into c-Si at 250 keV. All implants were performed with the sample heat sunk to a copper block cooled by liquid nitrogen. The pressure during implantation was below 10^{-7} mbar. The amorphous layer thicknesses and Er concentration profiles were measured with Rutherford backscattering spectrometry (RBS) using 2 MeV He. Thermal annealing and SPE were performed in either a rapid thermal annealer (RTA) under flowing Ar or in a standard tube furnace at a pressure below 10^{-7} mbar. IBIEC was performed using a 500 keV Si beam with a beam current on target of 2 μA. The sample was attached with silver paint to a copper block held at a constant temperature of 250°C. The total Si fluence was 8.9×10^{16} ions/cm^2 and the pressure during irradiation was 10^{-6} mbar.

Photoluminescence (PL) spectroscopy was performed using the 514.5 nm line of an Ar^+ laser as a pump source. The 1/e penetration depth of this wavelength is 890 nm in (defect-free) c-Si [20], and 28–44 nm in a-Si [21], depending on the degree of structural relaxation. Pump powers were either 200 or 300 mW, and the pump beam was mechanically chopped at 15 Hz (a-Si:Er) or 55 Hz (c-Si:Er). The luminescence signal was collected using a 0.5 m monochromator, a liquid nitrogen cooled Ge detector, and a lock-in amplifier. The spectral resolution was 6 nm. Low-temperature PL measurements were performed using a liquid nitrogen cooled cryostat, with the samples kept in vacuum (10^{-7} mbar). No absolute measurements were performed, but all PL spectra are plotted against the same ordinate, so relative intensities may be compared.

3. Results

3.1. Er in amorphous Si

RBS measurements (not shown) showed that the Er profile in the amorphized Si sample (250 keV, $5.4 \times$

10^{15} Er/cm^2) was Gaussian shaped, peaked at a depth of 80 nm, with a full width at half maximum of 60 nm. The Er peak concentration was 8×10^{20} cm^{-3} (1.6 at.%). PL measurements at 77 K did not show any measurable signal from the as-implanted sample. Thermal annealing of a-Si:Er is necessary to observe measurable PL. An optimum was found [22] after annealing at 400°C for 1 h. RBS shows no indications at this temperature for diffusion of Er, nor recrystallization of the a-Si layer. The PL spectrum, measured at 77 K, is shown in fig. 2. A broad background is observed, which is also seen in pure a-Si, which was not implanted with Er [22]. Superimposed on the a-Si band is the characteristic luminescence of Er with a main peak at 1.542 μm and a side peak at 1.553 μm.

3.2. SPE of a-Si:Er

Fig. 3 shows a RBS/channeling spectrum after implantation of 9×10^{14} Er/cm^2 in Si(100) at 250 keV. As can be seen, a continuous amorphous layer has formed; it extends from the surface to a depth of 160 nm. The as-implanted Er profile is approximately Gaussian and peaks at a depth of 70 nm, with a full width at half maximum of 60 nm. The Er peak concentration is 1.5×10^{20} cm^{-3}. Spectra for samples annealed at 600°C for 15 min or at 900°C for 15 s are also shown in fig. 3. After annealing at 600°C, the a-Si has epitaxially crystallized, leaving a thin disorder peak (10 nm) at the surface. The channeling minimum yield in the recrystallized layer is $\chi_{min} < 5\%$, indicating good crystal quality. The Er has been redistributed, with 65% of the Er remaining trapped in c-Si at a maximum concentration of 9×10^{19} cm^{-3}, and the remainder in the surface disordered layer. The Er profiles under

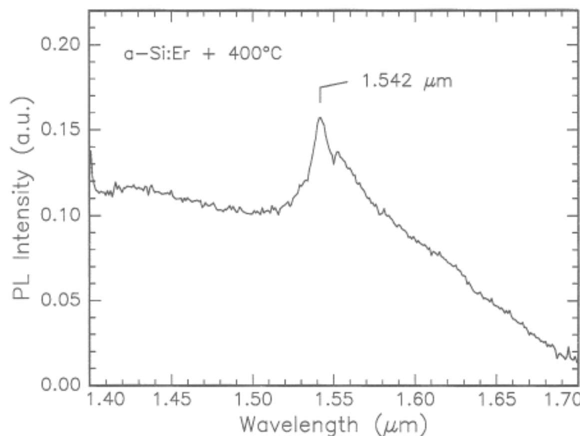

Fig. 2. Photoluminescence spectrum at 77 K for Er-doped amorphous Si (5.4×10^{15} Er/cm^2, 250 keV) after annealing at 400°C for 1 h. A 200 mW, 514.5 nm excitation source was used. Spectral resolution = 6 nm.

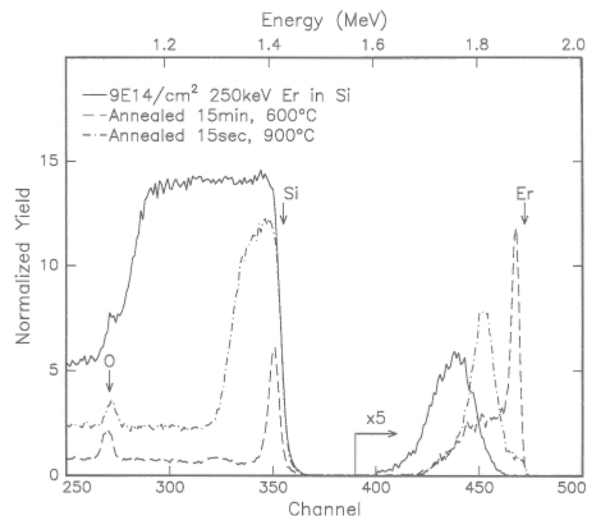

Fig. 3. RBS/channeling spectra for Er implanted Si (9×10^{14} cm^{-2}, 250 keV), after implantation and after subsequent solid phase crystallization at 600°C (15 min) or 900°C (15 s). The scattering angle was 100°.

channeling or random measuring condition were identical, so Er is not on substitutional lattice sites. The redistribution of Er during SPE is a result of segregation and trapping at the moving c-Si/a-Si interface. More detailed studies [23,24] show that during the segregation process Er is accumulating in an extremely narrow segregation spike at the moving c-Si/a-Si interface at concentrations as high as 10 at.%

In contrast, during 900°C annealing, the initial regrowth is first epitaxial, but 60 nm from the surface the quality of the regrowth deteriorates rapidly. Cross-section transmission electron microscopy has shown the formation of twins from the depth at which RBS shows the disordered layer [23]. In the epitaxial region (deeper than 60 nm), Er is trapped at concentrations similar to those for the 600°C anneal. Once damaged crystal growth begins, Er is trapped at higher concentrations possibly at the twin boundaries. The sample is recrystallized to the surface as evidenced from both the redistribution of some Er to the surface and the moderate channeling in the Si signal.

Fig. 4 shows PL spectra of Si:Er regrown by SPE at 600°C, measured at 77 K. The as-regrown sample shows clear PL with the spectrum peaked at 1.538 μm. Subsequent rapid thermal annealing at temperatures in the range 800–1300°C (15 s), causes a further increase in PL intensity; a maximum is reached for annealing at 1000°C. This spectrum is also shown; it is similar in shape but ≈ 3 times more intense than that of the as-grown sample. For both spectra in fig. 4 the main peak as well as the side peak at around 1.55 μm are attributed to transitions between different Stark levels

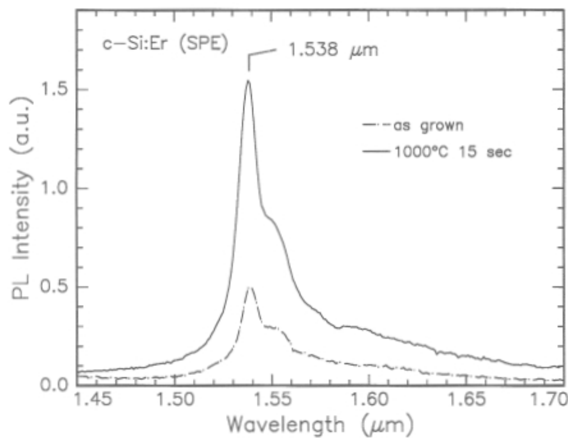

Fig. 4. Photoluminescence spectra at 77 K of c-Si doped with Er by SPE. A 160 nm layer was first amorphized by 9×10^{14} Er/cm^2 at 250 keV, and then crystallized using thermal annealing at 600°C for 15 min. Spectra are shown for the as-grown sample and after subsequent thermal annealing at 1000°C (15 s). A 300 mW, 514.5 nm excitation source was used. Spectral resolution = 6 nm.

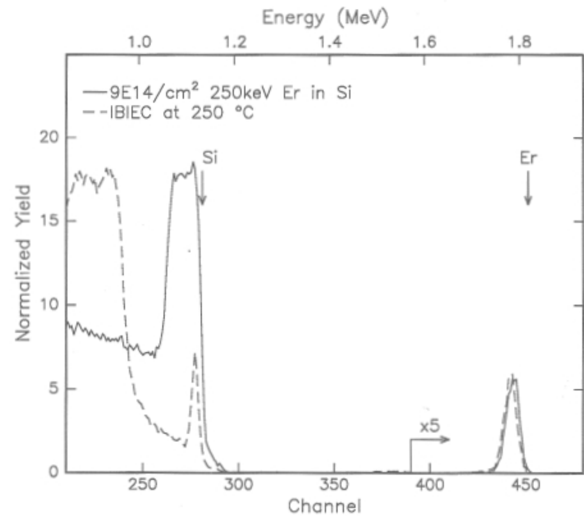

Fig. 6. RBS/channeling spectra for Er implanted Si (9×10^{14} cm^{-2}, 250 keV) after implantation, and after ion beam induced epitaxial crystallization at 250°C, using a 500 keV Si beam. The scattering angle was 169°.

(see arrows in fig. 1), which are homogeneously and inhomogeneously broadened. The asymmetry in the spectrum is explained by the fact that due to fast thermalization the emission proceeds mainly from the lowest lying level in the $^4I_{13/2}$ excited state term to the different Stark levels of the ground term, with the transition to the lowest level in the ground term being dominant.

Fig. 5 shows the PL peak intensity as a function of measuring temperature, plotted in an Arrhenius plot,

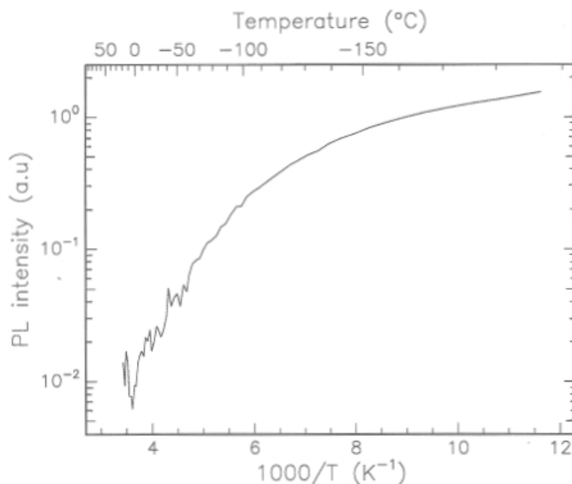

Fig. 5. Photoluminescence intensity at 1.539 μm as a function of temperature for the 1000°C annealed sample in fig. 4, plotted in an Arrhenius fashion. A 300 mW, 514.5 nm excitation source was used.

for the c-Si:Er sample regrown at 600°C and subsequently annealed at 1000°C. As can be seen, the PL intensity drops rapidly with increasing temperature, and finally at room temperature virtually no measurable signal is left. The activation energy which characterizes the temperature dependence of the PL intensity ranges from ~ 10–100 meV.

3.3. *IBIEC of a-Si:Er*

Fig. 6 shows RBS spectra of the Er-implanted sample after IBIEC. The spectrum for the as-implanted sample is also shown. The channeling spectrum after IBIEC shows that the a-Si has regrown to the surface with a < 20 nm thick disordered layer remaining at the surface. χ_{min} of the regrown layer is around 10%. A highly disordered region is observed in the spectrum below channel 250, corresponding to the damage caused by the Si beam during IBIEC. The most striking feature in fig. 6 is that the shape of the Er profiles before and after IBIEC is identical (the small shift is attributed to slight carbon buildup at the surface during IBIEC, which slightly shifts the surface channels). No segregation has occurred at the moving c-Si/a-Si interface. In this way an Er concentration as high as 1.5×10^{20} cm^{-3} was incorporated in crystal Si.

Fig. 7 shows PL spectra of Si:Er samples regrown by IBIEC, measured at 77 K. No PL was observed for the as-regrown sample. After subsequent annealing at 570°C a low-intensity PL spectrum is observed, with a maximum at 1.54 μm. The spectral width and asymmetry are quite similar to that measured for Si:Er crystal-

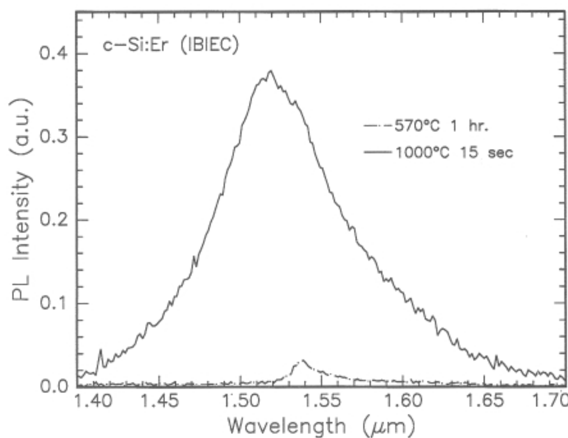

Fig. 7. Photoluminescence spectra at 77 K of c-Si doped with Er by IBIEC. A 160 nm layer was first amorphized by 9×10^{14} Er/cm^2 at 250 keV, and then crystallized using 8.9×10^{16} Si/cm^2 at 500 keV at 250°C. Spectra are shown after subsequent thermal annealing at 570°C (1 h) and 1000°C (15 s). A 300 mW, 514.5 nm excitation source was used. Spectral resolution = 6 nm.

lized by SPE at 600°C (fig. 4). However, if instead the sample is annealed at 1000°C, the spectrum is quite different; a broad and intense spectrum, peaked at 1.52 μm is observed.

4. Discussion

In section 3, three ways of incorporating Er in Si have been described. The simplest concept involves direct implantation of Er in amorphous Si. Doping a-Si may seem advantageous from a solubility point of view. As has been demonstrated for several transition metals [25–27], the effective solubility in a-Si is much higher than in c-Si, as a result of the presence of intrinsic defects and traps in the continuous random network structure of a-Si [28]. Typical solubilities found are in the order 10^{20} cm^{-3}. In the present experiments we have incorporated 8×10^{20} Er/cm^3. However, to obtain efficient light emission, Er has to be incorporated in the trivalent state, and it has to be excited efficiently. Earlier experiments have shown that the presence of oxygen is an essential prerequisite for the observation of Er photoluminescence (the O is supplied by the intrinsic O background of around 10^{18} cm^{-3} in CZ-Si) [6,7]. Possibly, Er and O form complexes in which Er has the required trivalent state. However, formation of such complexes generally requires annealing temperatures higher than the crystallization temperature of a-Si (≈ 600°C). Furthermore, excitation of Er requires the formation of electron–hole pairs with long enough lifetime and high enough mobility to reach the Er ions. Photocarrier lifetimes in a-Si are on the order of several ps [29], and the corresponding carrier diffusion lengths are negligible. Therefore only electron–hole pairs generated in the immediate vicinity of the Er ions can cause excitation of the Er. As the $1/e$ penetration depth of the pump laser is smaller than the projected range of the Er ions, only a very small fraction is excited, resulting in a low PL intensity. Finally, the high intrinsic defect concentration of a-Si may cause nonradiative decay of the excited Er ion, resulting in further quenching of the luminescence. The broad PL background in fig. 2 is attributed to transitions between energy levels in the a-Si band gap related these defects. Such defect luminescence is also seen in hydrogenated a-Si [30]. In contrast to what is seen in our experiments on pure a-Si, in Er-doped a-Si:H the defect luminescence intensity is smaller than that of the Er luminescence [9], as a result of the defect passivation by hydrogen.

In crystalline Si, the Er concentration which can be incorporated is smaller than in a-Si. As shown in fig. 3, for 600°C annealing, up to 9×10^{19} Er/cm^3 is trapped in the segregation process during SPE. More extensive experiments [23] have shown that for higher-fluence implants the regrowth eventually breaks down if the Er concentration in the crystal exceeds $(1.2 \pm 0.2) \times 10^{20}$ cm^{-3}. This limit is temperature dependent: for 900°C annealing it amounts to $(6 \pm 2) \times 10^{19}$ cm^{-3} [24]. This explains the breakdown seen during 900°C annealing in fig. 3. While thermal solid phase epitaxy of pure a-Si leads to complete recrystallization without breakdown over the entire temperature range from 450 to 1350°C [18] these data clearly show that the choice of annealing temperature is critical for recrystallizing Er-doped a-Si. This explains why earlier attempts to use SPE to incorporate high concentrations of Er in defect-free c-Si have failed, generally because too high a temperature was used during crystallization in an attempt to optically activate the Er in the same anneal step [13–16].

The PL intensity of the Si:Er sample grown by SPE is much higher than that of a-Si:Er, and it can be further enhanced by thermal annealing at 1000°C. We attribute this enhancement to the formation of Er–O complexes, an increase in the carrier lifetime, and/or the formation of Er-defect complexes which mediate the energy transfer from electron–hole pairs to the Er ion.

The advantage of IBIEC over SPE is that the Er profile remains unaltered after epitaxial regrowth. This is a result of the low annealing temperature (250°C) at which the Er mobility near the interface is too low for any redistribution to occur. On the other hand, IBIEC does not lead to a crystal quality as good as after SPE ($\chi_{min} = 10\%$). The broad PL spectrum observed after 1000°C annealing is completely different than that ob-

served after SPE with subsequent annealing at 1000°C. More measurements are needed to determine the precise nature of the broad band; it may originate from the Er, with the large width resulting from large inhomogeneous broadening due to the high Er concentration, or it may not be related to Er at all, but instead to defects in the Si crystal structure [31].

5. Conclusions

Three different ways of incorporating optically active Er in Si by ion implantation have been demonstrated. In pure amorphous Si, the characteristic luminescence at 1.54 μm is observed, superimposed on a broad defect–luminescence band from the a-Si itself. Due to the shallow pump penetration depth, small carrier lifetimes, and to the limit to the annealing temperature which can be used in a-Si, only a very low PL intensity is observed at 77 K.

Er concentrations up to $\approx 10^{20}$ cm^{-3} can be incorporated in crystal Si by SPE at 600°C or IBIEC at 250°C. SPE leads to good crystal quality ($\chi_{min} = 5\%$), but part of the Er segregates to the surface. During IBIEC the Er profile remains unaltered, but the crystal quality is not as good ($\chi_{min} = 10\%$). In both cases thermal annealing at 1000°C is necessary to optimize the PL intensity. While the integral PL intensities are similar for SPE or IBIEC samples, the spectrum after IBIEC is much broader. Absolute quantum efficiency measurements are necessary to further assess the usefulness of these optically doped materials: If all Er can be made optically active with a high fluorescence efficiency, Si-based light-emitting diodes, optical amplifiers, and lasers with useful output powers may be fabricated [32].

Acknowledgements

This work is part of the research program of the Foundation for Fundamental Research on Matter (FOM) and was made possible by financial support from the Dutch Organization for the Advancement of Pure Research (NWO), the Netherlands Technology Foundation (STW) and the IC Technology Program (IOP Electro-Optics) of the Ministry of Economic Affairs.

References

[1] A.M. Glass, Science 135 (1987) 1003.
[2] H. Ennen, J. Schneider, G. Pomrenke and A. Axmann, Appl. Phys. Lett. 43 (1983) 943.
[3] H. Ennen, G. Pomrenke, A. Axman, K. Eisele, W. Haydl and J. Schneider, Appl. Phys. Lett. 46 (1985) 381.
[4] D. Moutonnet, H. l'Haridon, P.N. Favennec, M. Salvi, M. Gauneau, F. Arnaud d'Avitaya and J. Chroboczek, Mater. Sci. Eng. B4 (1989) 75.
[5] Y.S. Tang, K.C. Heasman, W.P. Gillin and B.J. Sealy, Appl. Phys. Lett. 55 (1989) 432.
[6] J. Michel, J.L. Benton, R.F. Ferrante, D.C. Jacobson, D.J. Eaglesham, E.A. Fitzgerald, Y.-H. Xie, J.M. Poate and L.C. Kimerling, J. Appl. Phys. 70 (1991) 2672.
[7] P.N. Favennec, H. l'Haridon, D. Moutonnet, M. Salvi and M. Gauneau, Jpn. J. Appl. Phys. 29 (1990) L524.
[8] S. Schmitt-Rink, C.M. Varma and A.F.J. Levi, Phys. Rev. Lett. 66 (1991) 2782.
[9] T. Oestereich, C. Swiatowski and I. Broser, Appl. Phys. Lett. 56 (1990) 446.
[10] J.L. Benton, J. Michel, L.C. Kimerling, D.C. Jacobson, Y.-H. Xie, D.J. Eaglesham, E.A. Fitzgerald and J.M. Poate, J. Appl. Phys. 70 (1991) 2667.
[11] F.P. Widdershoven and J.P.M. Naus, Mater. Sci. Eng. B4 (1989) 71.
[12] Y.S. Tang and B.J. Sealy, Nucl. Instr. and Meth. B55 (1991) 647.
[13] D.J. Eaglesham, J. Michel, E.A. Fitzgerald, D.C. Jacobson, J.M. Poate, J.L. Benton, A. Polman, Y.-H. Xie and L.C. Kimerling, Appl. Phys. Lett. 58 (1991) 2797.
[14] Y.S. Tang and Zhang Jingping, J. Crystal Growth 102 (1990) 681.
[15] W.P. Gillin, Zhang Jingping and B.J. Sealy, Solid State Commun. 77 (1991) 907.
[16] Y. Yan, Q. Li, D. Feng, P. Wang and H. Sun, Mater. Lett. 7 (1989) 445.
[17] R.J. Schreutelkamp, J.S. Custer, J.R. Liefting, W.X. Lu and F.W. Saris, Mater. Sci. Rep. 6 (1991) 275.
[18] G.L. Olson and J.A. Roth, Mater. Sci. Rep. 3 (1988) 1.
[19] F. Priolo and E. Rimini, Mater. Sci. Rep. 5 (1990) 319.
[20] G.E. Jellison and F.A. Modine, J. Appl. Phys. 53 (1982) 3745.
[21] M. Fried, T. Lohner, W.A.M. Aarnink, L.J. Hanekamp and A. van Silfhout, J. Appl. Phys. 71 (1992) 5260.
[22] J.S. Custer, E. Snoeks and A. Polman, Mater. Res. Soc. Symp. Proc. 235 (1992) 51.
[23] A. Polman, J.S. Custer, E. Snoeks and G.N. van den Hoven, Appl. Phys. Lett., in press.
[24] A. Polman, J.S. Custer, E. Snoeks and G.N. van den Hoven, to be published.
[25] A. Polman, D.C. Jacobson, S. Coffa, J.M. Poate, S. Roorda and W.C. Sinke, Appl. Phys. Lett. 47 (1990) 1230.
[26] S. Coffa, J.M. Poate, D.C. Jacobson and A. Polman, Appl. Phys. Lett. 58 (1991) 916.
[27] J.S. Custer, M.O. Thompson and J.M. Poate, Mater. Res. Soc. Symp. Proc. 128 (1989) 545.
[28] S. Roorda, W.C. Sinke, J.M. Poate, D.C. Jacobson, S. Dierker, B.S. Dennis, D.J. Eaglesham, F. Spaepen and P. Fuoss, Phys. Rev. B44 (1989) 3702.
[29] P.A. Stolk, L. Calcagnile, S. Roorda, W.C. Sinke, A.J.M. Berntsen and W.F. van der Weg, Appl. Phys. Lett. 60 (1992) 1688.
[30] R.A. Street, Phys. Rev. B21 (1980) 5775.
[31] G. Davies, Phys. Rep. 176 (1989) 83.
[32] Y.-H. Xie, E.A. Fitzgerald and Y.J. Mii, Appl. Phys. Lett. 70 (1991) 3223.